

Effects of surface conditions on resistance spot welding of Mg alloy AZ31

L. Liu^{*1,2}, S. Q. Zhou^{1,3}, Y. H. Tian², J. C. Feng², J. P. Jung^{1,4} and Y. N. Zhou¹

In this work, resistance spot welding of Mg alloy AZ31 sheets was investigated in as received and acid cleaned surface conditions. As received sheets had higher contact resistance which required lower current thresholds for weld initiation and for four root t nugget size (where t is sheet thickness). However, it also led to both serious expulsion and internal defects. The fracture mode of welds in as received sheets was interfacial failure while that of the acid cleaned specimens shifted from interfacial to nugget pullout and exhibited better strength. The acid cleaned sheets also produced less damage on electrode tip faces.

Keywords: Surface condition, Contact resistance, Magnesium alloy, Resistance spot welding

Introduction

In recent years, magnesium (Mg) alloys, with their high strength to weight ratio, good damping capacity and easy recycle, have attracted great attention in engineering research and have been employed in automotive industry applications to produce lightweight vehicles.¹ Mg alloys may be welded by a number of processes including gas tungsten arc, electron beam, laser, friction stir, explosion and resistance spot welding.²⁻⁵ However, the properties of Mg alloys such as high thermal conductivity, low surface tensions, low boiling temperature and low absorptivity of laser beams would easily produce defects such as weld drop-through, pores, cracks and oxide inclusion.⁶ Resistance spot welding (RSW) is a primary joining method in the auto industry due to its ability to assemble thin sheets, in which many defects could be avoided such as weld drop-through.⁵ Also no fillers are needed, which is important since it is not easy to produce commercial Mg welding wire due to its poor formability.⁷ However, despite the ever increasing demands to use RSW to join Mg alloys, only few feasibility studies have been published and detailed investigations such as on the effects of surface conditions are needed.⁸⁻¹¹

It is expected that surface conditions (roughness, oxide films and other contaminants) would have great influences on RSW of Mg alloys.¹² Surface conditions would alter contact resistance and hence ohmic heating generated at the faying surfaces. Since the Mg bulk resistance is relatively low, this could be the critical energy resource to melt material, similar to RSW of Al

alloys.^{5,12} If the contact resistance is too high, e.g. caused by thick oxide films as in Al alloys,¹² too much energy could lead to expulsion or other defects. Surface roughness might induce sliding on the microscopic scale and lead to breaking down contact resistance.¹³ Also ohmic heating at the electrode/sheet surface, again affected by surface conditions, would lead to electrode degradation as in RSW of Al alloys.¹⁴

The objective of the current work was to investigate the influence of surface conditions on the weldability of AZ31 magnesium alloy in terms of weld nugget growth, surface expulsion, joint strength and electrode tip face stability.

Materials and experimental procedure

Magnesium alloy AZ31 (Table 1) sheets with a thickness of 2 mm were used in the present study. Lap welded joints were made by assembling test coupons which were cut to approximately 25 mm width and 100 mm length. Specimens were cut parallel to the rolling direction of the sheets and cleaned first by ultrasonic cleaning machine with acetone to remove oil. To investigate the influence of surface condition, three different surface conditions were used for welding. Surface conditions varied significantly on as received sheets, even from the same package. For example, some surface areas looked bright and others looked dark. Therefore, two as received surface conditions were designated as AR-W (white) and AR-B (black). Another surface condition was created by 2.5% (w/v) chromic acid cleaning of as received and acetone washed sheets.

Specimens were welded using a single phase ac spot welding machine in the constant current mode. Welding

¹Centre for Advanced Materials Joining, University of Waterloo, Waterloo, Ont., Canada

²State Key Laboratory of Advanced Welding Production Technology, Harbin Institute of Technology, Harbin, China

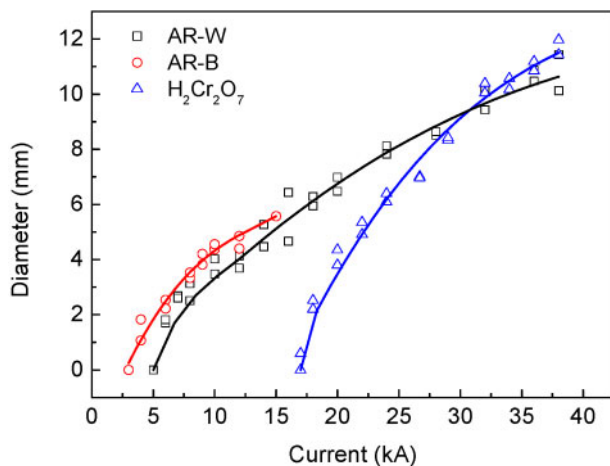
³School of Mechanical Science and Engineering, Huazhong University of Science and Technology, Wuhan, China

⁴Department of Materials Science and Engineering, University of Seoul, Seoul, Korea

*Corresponding author, email rayliu@engmail.uwaterloo.ca

Table 1 Nominal chemical composition of AZ31 alloy

Al	2.92
Zn	1.09
Mn	0.3
Si	0.01
Mg	Bal.



1 Weld nugget diameter v. welding current at different surface conditions

conditions were the same for all the three surface conditions as listed in Table 2. Five welding samples were made under each welding condition: two for the measurement of nugget diameter and three for tensile shear test. All Mg tensile coupons were strained to fracture at a constant crosshead speed of 1 mm min^{-1} . Maximum load was used to indicate the strength of welds.

Surface roughness was investigated using a Wyko NT1100 instrument. Contact resistance of faying surface was measured using a DLRO-10X Digital Low Resistance Ohmmeter (AVO International Ltd), in which 4 kN electrode force was applied without welding current. The reported values of surface roughness and contact resistance are averages of 10 and 20 nominally identical measurements respectively. Electrode tip faces were investigated by JEOL JSM 840, scanning electron microscopy/energy dispersive X-ray spectroscopy (SEM/EDS) with 20 kV operating voltage in the as welded condition.

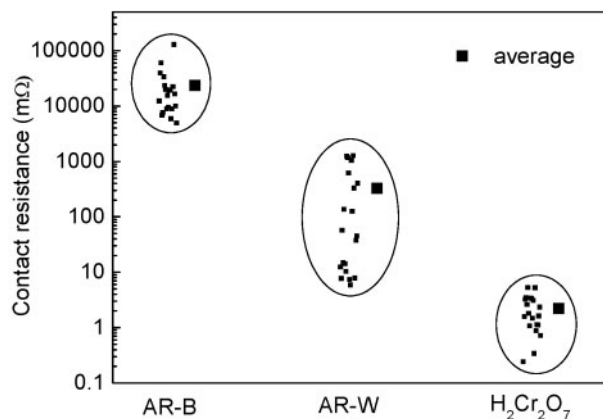
Results and discussion

Nugget diameter and surface expulsion

Figure 1 shows the measured nugget diameter v. welding current for different surface conditions, which confirms that nugget diameter increased with increasing welding current. When current was higher than 30 kA, the nugget size of the AR-W sheets was found to be nearly the same as the acid cleaned sheets. It was also seen that surface conditions affected the current threshold for weld initiation, which was defined as the first visual observation of melting at the faying surface.^{15,16} Chromic acid cleaned coupons exhibited the largest threshold current while AR-B sheets exhibited the smallest, which is believed to be related to the contact resistance as indicated below.

Table 2 Welding conditions

Welding parameter	Value
Electrode force, kN	4
Welding current, kA	3–38
Welding time	1–20 cycles at 60 Hz
Holding time	30 cycles at 60 Hz
Electrode type	FF-25



2 Contact resistances of different surface conditions

The effect of surface condition on contact resistance is shown in Fig. 2. Owing to the wide range of resistance values measured with different surface conditions, the contact resistance points are plotted with semilogarithmic scales. The AR-B condition produced the highest contact resistance, which was about two orders of magnitude above that of the AR-W condition, and about four orders above that of the chromic acid cleaned condition.

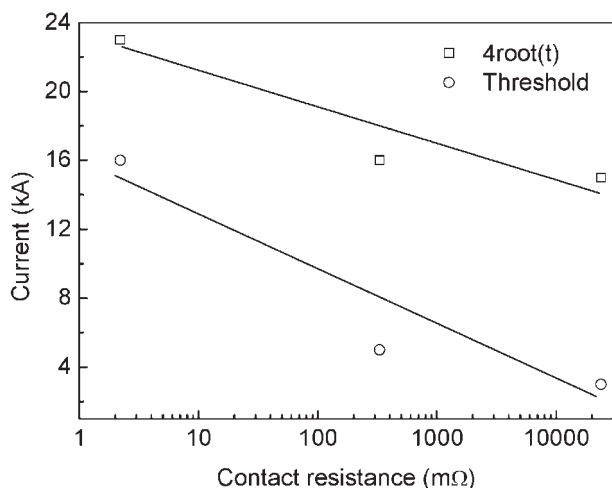
Table 3 shows the roughness average (Ra) of different surface conditions. The Ra of the three surfaces was generally at the same level. It can be seen that the two as received conditions both had higher standard deviation indicating non-uniform surfaces. Acid cleaning made the surface roughness more uniform.

For most engineering materials, the contact resistance includes both the constriction and film resistances.^{17,18} Since the differences of Ra values at the three surface conditions were not significant (Table 3), the contact resistance in this work is believed to be mainly affected by the oxide layer thickness, which is very similar to the situation in RSW of Al alloys.^{12,13} Mg alloys can be easily oxidised during manufacture because of the hot rolling process.¹⁹ Local oxidation can also be promoted by dampness during shipping or storage. Therefore, as received surface conditions are sensitive to the process and environmental variations. Black colour may be an indication of serious oxidation as compared with the white and shiny colour. The acid used in this work clearly reduced oxide layer thickness, which produced the lowest contact resistance.

Figure 3 shows influence of contact resistance on the threshold current for weld initiation and for the formation of $4t^{1/2}$ nugget size welds, where t is sheet thickness. It appears that the required current decreased linearly with semilogarithmic resistance. A similar result was shown by Savage *et al.*,¹⁶ in which pickled steel (low contact resistance) started to show melting at 9450 A, while the uncleaned steel started to melt at 5850 A. Chang and Zhou's study on the effect of welding force

Table 3 Surface roughness

Surface conditions	Ra, nm	Standard deviation, nm
AR-B	562	203
AR-W	684	128
H ₂ Cr ₂ O ₇	680	68



3 Welding current v. contact resistance

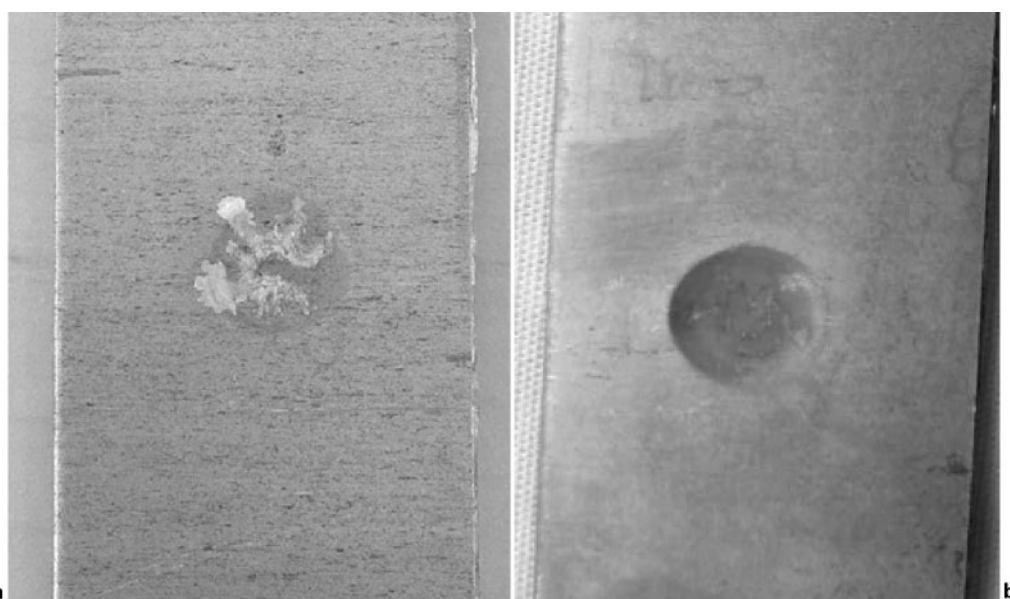
on the threshold current found that increasing welding force can increase threshold current due to reduction of contact resistance.¹⁵ In resistance spot welding, a certain level of contact resistance is beneficial to the formation of welds since sufficient ohmic heating could be produced for the initiation and nugget growth in the early stage of welding, as pointed out by Han *et al.*²⁰ On the other hand, a higher contact resistance at the electrode/workpiece interface is also helpful to create a thermal blanket effect that keeps the heat generated from the workpiece faying surface within the workpiece. This is why chromic acid cleaned specimens need larger current to form initial welds. However, above 30 kA, nugget sizes of the different surface conditions were nearly the same under the same welding current (Fig. 1). This could be because at lower current, the fraction of heat generated by bulk resistance was low. With higher currents, bulk resistance, which is unrelated to surface condition, produced more of the total heat, thus making the nugget sizes in welds with different surface conditions more similar.

However, if contact resistance is too high, rapid heating could lead to surface expulsion as shown in Fig. 4. Variation of surface conditions has a significant influence on the risk of expulsion at the sheet/electrode interface. No surface expulsion was found even when current was as high as 26 kA for chromic acid cleaned surfaces (Fig. 4b). However, serious surface expulsion for AR-W surface condition was found with the same current (Fig. 4a). The worst performance was with the AR-B sheets, in which when the current was higher than 15 kA, serious expulsion blew a hole in the sheets, as shown in Fig. 5.

Joint strength

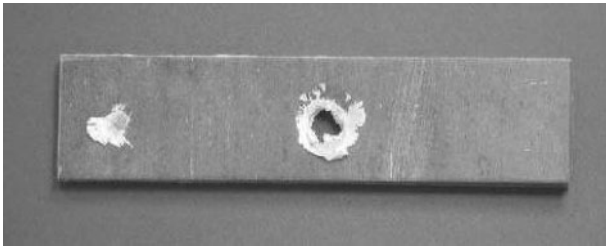
The following discussion focuses on the joint strength of AR-W and chromic acid cleaned surfaces, due to the poor weldability of the AR-B condition. Figure 6 shows the influence of nugget size on the shear strength with different surface conditions: increasing nugget diameter appeared to increase shear force. It is interesting to note that, for the same nugget size, shear forces of chromic acid cleaned specimens were higher than those of the AR-W. When nugget diameter was above 10 mm, the fracture mode of chromic acid cleaned specimens shifted from interfacial to nugget pullout, whereas the AR-W welds all displayed interfacial failure. This difference in fracture behaviour may be related to the amount of internal porosity, as shown in Fig. 7. The AR-W welds showed more porosity than the acid cleaned welds.

It has been pointed out by numerical modelling that higher pore percentage will reduce the strength of welds.²¹ Also, according to the study of Wang *et al.*,⁸ high contact resistance caused by oxide films leads to rapid melting and hence violent ejection (faying surface expulsion) of the material. That in turn may lead to a shortage of material to fill the voids during the subsequent solidification. Moreover, since the boiling temperature of magnesium is as low as $\sim 1000^{\circ}\text{C}$,²² loss of material by vaporisation may also happen during welding especially because of the high heat generation at the faying surface with high contact resistance. Furthermore, the oxide layer of Mg alloys is very

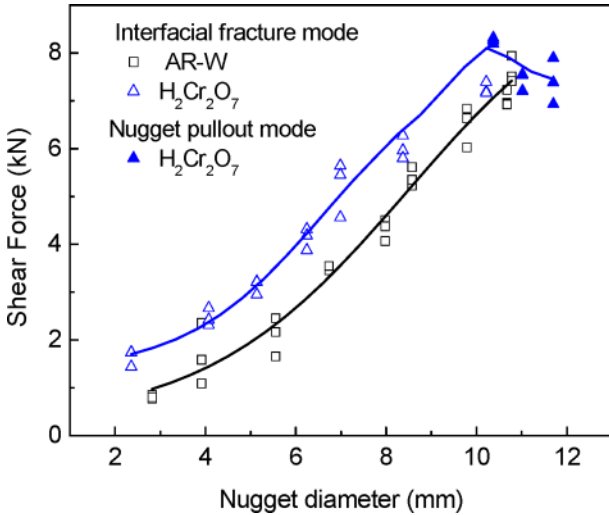


a AR-W; b $\text{H}_2\text{Cr}_2\text{O}_7$

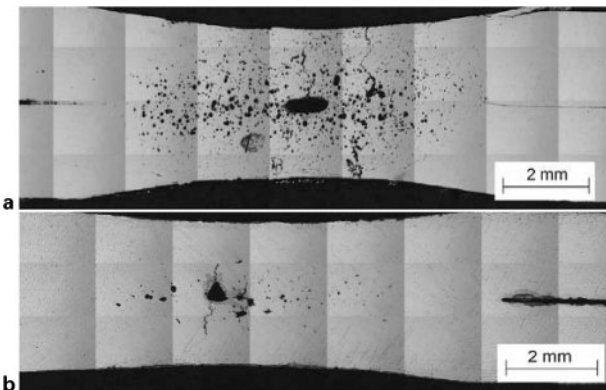
4 Sheet surfaces after welding at 26 kA



5 Blow-through hole of AR-B condition



6 Shear force as function of different nugget diameters at different surface conditions



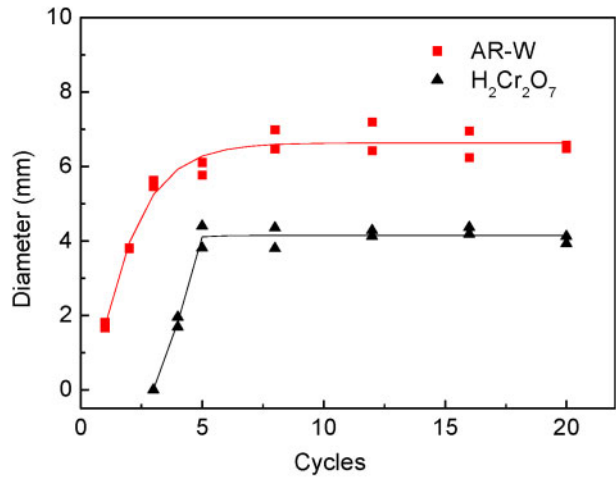
a AR-W; b acid cleaned

7 Cross-sections of welds with nearly 9 mm diameter nuggets at different surface conditions showing varied porosities

reactive with H₂O,²³ which could lead to hydrogen pores inside the nugget if excessive surface oxide is present before welding.

Welding time

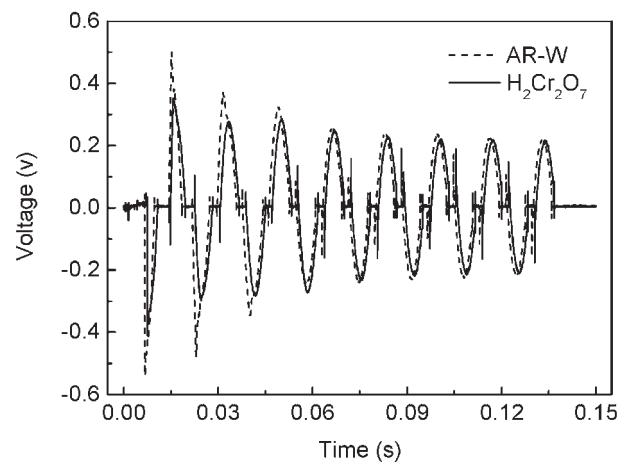
Figure 8 shows the relationship of nugget diameter and welding cycles when welding current was 20 kA. The nugget diameter increases initially with increasing welding cycles but levels off after five cycles. This is similar to RSW of aluminium, in which required welding time is relatively short because of the higher thermal conductivity and more important role of contact resistance as compared with RSW of steels.²⁴ Again,



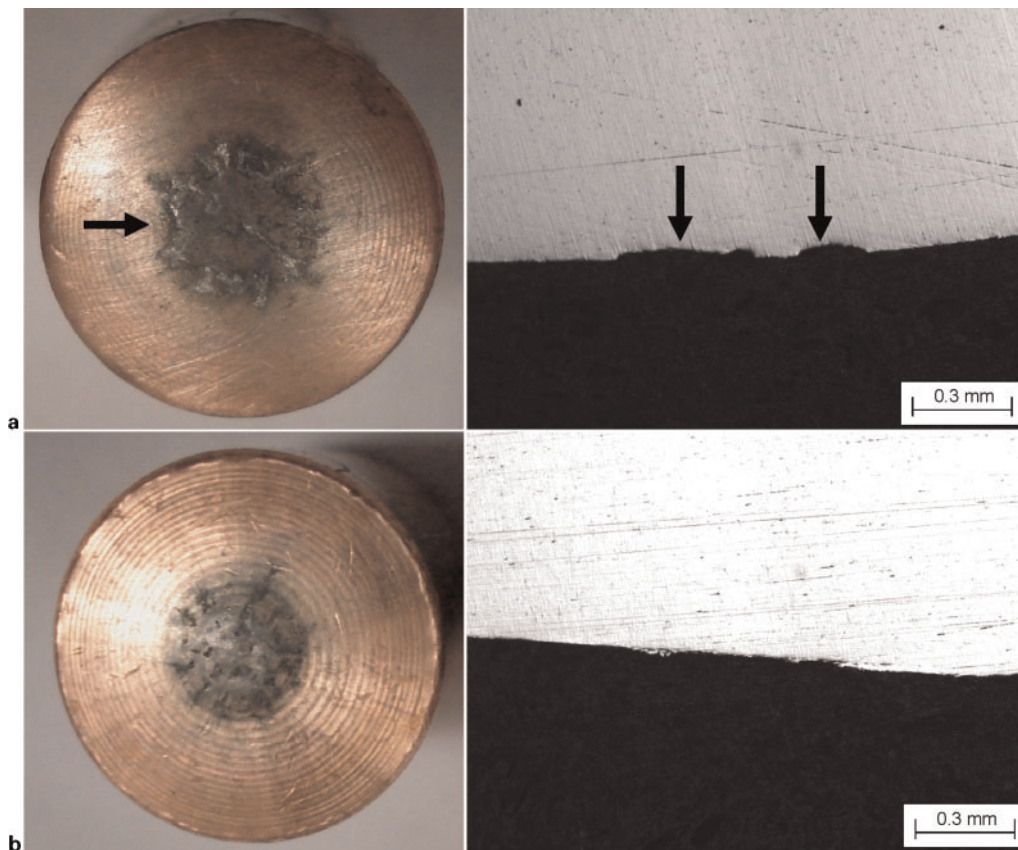
8 Nugget diameter v. welding cycles

the AR-W condition produced larger nugget size because of the higher contact resistance compared with the acid cleaned sheets. The largest difference was found at three cycles, in which the AR-W nugget size was ~5.5 mm while acid cleaned coupons still had no nugget formed. This relationship of nugget size and welding time can also be understood through the heat generation at the faying surfaces as described below.

Because of the phase shift between measured current and voltage, it is difficult to calculate the precise value of energy input of ac resistance spot welding. However, since the measured RMS current values of AR-W and acid cleaned sheets were nearly the same at 19.15 and 19.07 kA respectively, the voltage drop at the faying surface, as shown in Fig. 9, can be used to indicate the differences in dynamic resistance and heat generation between the two conditions. It can be seen that the voltage of AR-W coupons was higher than that of acid cleaned coupons during the first three cycles, after which both voltage drops were stable and nearly the same. This means that the dynamic resistance and heat generation of the AR-W condition were higher than those of the acid cleaned sheets only during the first three cycles. The dynamic resistance during RSW is the result of the changes in bulk resistance and contact resistance.¹⁸ Compared with film resistance, the bulk resistance is relatively low due to the high electrical conductivity of magnesium alloy. Therefore, the heat caused by the film

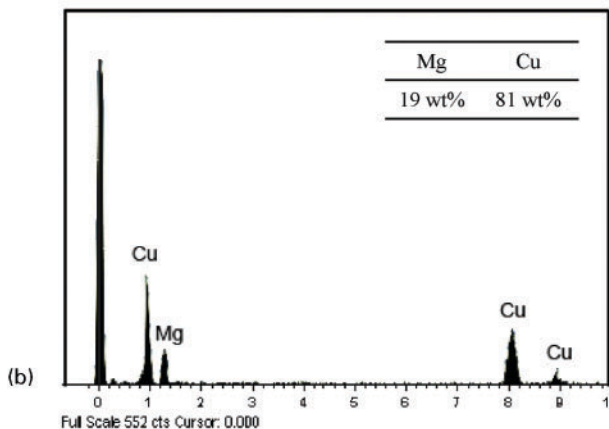
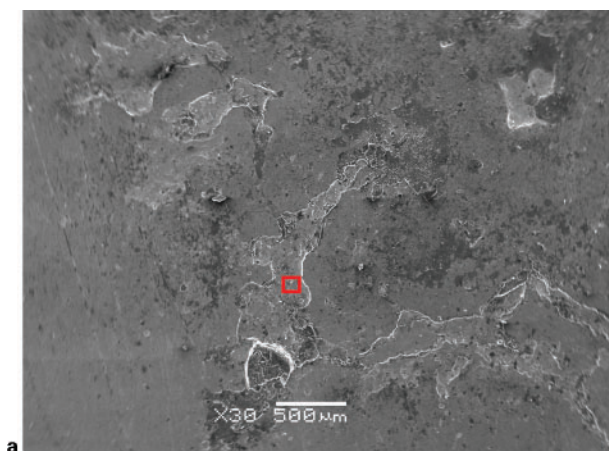


9 Voltage drop across faying surface



a AR-W; b H₂Cr₂O₇

10 Electrode tip faces of a as received and b acid cleaned conditions: heavy pits were indicated by arrows



11 a micrograph (SEM) of surface damage on electrode tip faces when welding AR-W sheets and b EDS spectrum and composition of highlighted area in a

resistance is the main heat source in RSW of Mg alloys. During welding, after the breakdown of surface films, the subsequent heat generation would be similar for both surface conditions.

Electrode tip faces

Surface conditions would also affect the life of electrodes. The AR-W and chromic acid cleaned sheets were selected for comparison of the electrode tip face quality. After 40 welds made at welding parameters of 28 kA and eight cycles, much more surface damage (large pitted areas) was found on the electrode tip faces at the AR-W condition as shown in Fig. 10. The EDS analysis shows that the pitted areas had a surface composition of 19 wt-%Mg and 81 wt-%Cu (Fig. 11), indicating that the sheet material (AZ31) transferred onto the tip face. Similar to the behaviour in RSW of aluminium alloys,¹⁴ higher contact resistance would increase Mg pick-up and alloying with the copper electrode and hence speed up the electrode degradation.

Conclusions

Resistance spot welding was performed on Mg alloy AZ31 sheets in as received and acid cleaned surface conditions. It was found that as received surfaces had very high contact resistance with large variations. The higher contact resistance produced lower welding current thresholds for weld initiation and for the formation of four root *t* nugget size, but led to both serious expulsion and internal porosity.

Acid cleaning produced much more uniform surfaces with lower contact resistance, which resulted in higher

shear strength with the same weld size because of lower percentage of internal nugget porosity. When the welding current was above 34 kA, the fracture mode shifted from interfacial to nugget pullout while that of the as received sheets remained as interfacial. The lower contact resistance also caused less damage to the electrode tip faces and less Mg pick-up.

Acknowledgment

The authors would like to acknowledge the funding and support from Auto21 (<http://www.auto21.ca>), one of the Networks of Centres of Excellence supported by the Canadian Government.

References

1. G. Song, L. Liu and P. Wang: *Mater. Sci. Eng. A*, 2006, **A429**, (1–2), 312–319.
2. Z. Sun, D. Pan and J. Wei: *Sci. Technol. Weld. Join.*, 2002, **7**, (6), 343–351.
3. C. T. Chi, C. G. Chao, T. F. Liu and C. C. Wang: *Sci. Technol. Weld. Join.*, 2008, **13**, (2), 199–211.
4. A. Gerlich, P. Su and T. H. North: *Sci. Technol. Weld. Join.*, 2005, **10**, (6), 647–652.
5. Y. R. Wang, Z. H. Mo, J. C. Feng and Z. D. Zhang: *Sci. Technol. Weld. Join.*, 2007, **12**, (8), 671–676.
6. X. Cao, M. Jahazi, J. P. Immarrigeon and W. Wallace: *J. Mater. Process. Technol.*, 2006, **171**, (2), 188–204.
7. J. Valle, F. Carreño and O. Ruano: *Acta Mater.*, 2006, **54**, (16), 4247–4259.
8. Y. R. Wang, J. C. Feng and Z. D. Zhang: *J. Mater. Sci. Technol.*, 2005, **21**, (5), 749–752.
9. J. C. Feng, Y. R. Wang and Z. D. Zhang: *Sci. Technol. Weld. Join.*, 2006, **11**, (2), 154–162.
10. D. Q. Sun, B. Lang, D. X. Sun and J. B. Li: *Mater. Sci. Eng. A*, 2007, **A460–A461**, (15), 494–498.
11. Y. R. Wang, J. C. Feng and Z. D. Zhang: *Sci. Technol. Weld. Join.*, 2006, **11**, (5), 555–560.
12. T. Ronnhult, U. Rilby and I. Olefjord: *Mater. Sci. Eng.*, 1980, **42**, 329–336.
13. E. Crinon and J. T. Evans: *Mater. Sci. Eng. A*, 1998, **A242**, (1), 121–128.
14. I. Lum, S. Fukumoto, E. Biro, D. R. Boomer and Y. Zhou: *Mater. Trans. A.*, 2004, **35A**, 217–226.
15. B. H. Chang and Y. Zhou: *J. Mater. Process. Technol.*, 2003, **139**, (1–3), 635–641.
16. W. F. Savage, E. F. Nippes and F. A. Wassell: *Weld. J.*, 1978, **57**, 43s–50s.
17. S. C. Wang and P. S. Wei: *J. Heat Transfer*, 2001, **123**, (3), 576–585.
18. W. Tan, Y. Zhou, H. W. Kerr and S. Lawson: *J. Phys. D, Appl. Phys.*, 2004, **37D**, 1998–2008.
19. H. Watari, T. Haga, N. Koga and K. Davey: *J. Mater. Process. Technol.*, 2007, **192–193**, (1), 300–305.
20. J. H. Han, P. Shan and S. S. Hu: *Mater. Sci. Eng. A*, 2006, **A435–A436**, (5), 204–211.
21. J. Zhang and P. Dong: *Eng. Fract. Mech.*, 1998, **59**, (6), 815–825.
22. J. Senkara, H. Zhang and S. J. Hu: *Weld. J.*, 2004, **83**, (4), 123s–132s.
23. N. H. Leeuw, G. W. Watson and S. C. Parker: *J. Chem. Soc., Faraday Trans.*, 1996, **92**, 2081–2091.
24. Y. Cho, S. J. Hu and W. Li: *Proc. Inst. Mech. Eng. B, J. Eng. Manuf.*, 2003, **217B**, (10), 1355–1363.